

PyCDFT: A Python package for constrained density functional theory

He Ma^{*†}, Wennie Wang[‡], Siyoung Kim[‡], Man-Hin Cheng^{‡§},
Marco Govoni^{†‡}, Giulia Galli^{*†‡}

Abstract

We present PyCDFT, a Python package to compute diabatic states using constrained density functional theory (CDFT). PyCDFT provides an object-oriented, customizable implementation of CDFT, and allows for both single-point self-consistent-field calculations and geometry optimizations. PyCDFT is designed to interface with existing density functional theory (DFT) codes to perform CDFT calculations where constraint potentials are added to the Kohn-Sham Hamiltonian. Here we demonstrate the use of PyCDFT by performing calculations with a massively parallel first-principles molecular dynamics code, **Qbox**, and we benchmark its accuracy by computing the electronic coupling between diabatic states for a set of organic molecules. We show that PyCDFT yields results in agreement with existing implementations and is a robust and flexible package for performing CDFT calculations. The program is available at <https://github.com/hema-ted/pycdft/>.

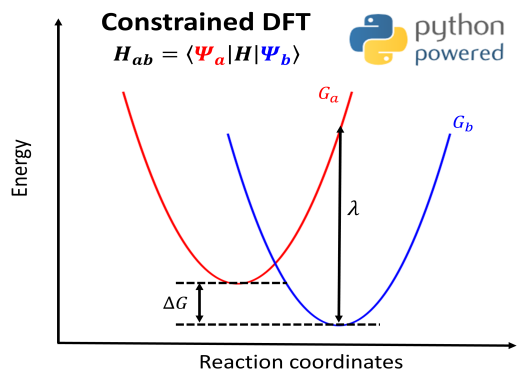
Keywords: constrained density functional theory, charge transfer, electronic coupling, diabatic states, Python ■

^{*}Department of Chemistry, University of Chicago, Chicago, Illinois 60637, United States

[†]Materials Science Division and Center for Molecular Engineering, Argonne National Laboratory, Lemont, Illinois 60439, USA

[‡]Pritzker School of Molecular Engineering, University of Chicago, Chicago, Illinois 60637, United States

[§]Current Address: Department of Physics, ETH Zurich, 8093 Zurich, Switzerland



Charge transfer plays a critical role in many physical, chemical, and biological processes, and can be described using the coupling between diabatic states. In this work, we present PyCDFT, an open-source Python package that is robust, flexible, and DFT-engine agnostic for calculating diabatic states and their electronic coupling using constrained density functional theory.

1 INTRODUCTION

The transfer of electronic charges plays a central role in many physical and chemical processes¹, such as those for cellular activity in biological processes² and catalytic activity in condensed phases³. In addition, the rate of charge transfer in a material directly impacts its carrier mobility and hence its use in e.g., electronic devices^{4,5}.

Theoretical and computational modeling provides invaluable insights into the microscopic mechanism of charge transfer, and is playing an important role in the development of novel drugs, catalysts, and electronic materials. In the past few decades, many research efforts have been dedicated to the development of robust theoretical methods and simulation strategies to describe charge transfer processes in molecules and materials^{6–12}. Charge transfer can take place through a wide spectrum of mechanisms, with two important regimes being the band-like regime (where transport occurs through delocalized electronic states) and the hopping regime (where transport occurs through localized electronic states)^{13,14}. Here we focus on the hopping transfer, which is the dominant charge transfer mechanism in many organic crystals and conducting polymers, and in several metal oxides in the solid state, as well as in many nanoparticle solids^{15–18}.

The classic theory of charge transfer in the hopping regime is Marcus theory^{19,20}, which has seen many generalizations through the years^{21–24}. For a charge transfer between two sites A and B (e.g., a donor-acceptor pair consisting of two molecules or two fragments of the same molecular unit), Marcus theory predicts the charge transfer rate to be

$$k = \frac{2\pi}{\hbar} |H_{ab}|^2 \sqrt{\frac{1}{4k_B T \pi \lambda}} \exp \left[-\frac{(\Delta G + \lambda)^2}{4\lambda k_B T} \right], \quad (1)$$

where the diabatic electronic coupling H_{ab} between A and B is one of the central quantities that determines transfer rates; k_B and T are the Boltzmann constant and temperature; ΔG is the free energy difference between states A and B, and λ is the reorganization energy. As shown in Fig. 1, within Marcus theory the charge transfer process can be described using the free energy surfaces of two *diabatic states* as functions of a chosen reaction coordinate. Diabatic states are defined as a set of states among which the nonadiabatic derivative couplings vanish. Diabatic states have the property that their physical characters (such as charge localization) do not change along the reaction coordinate. For instance, the two diabatic

states (Ψ_a/Ψ_b) involved in the charge transfer depicted in Fig. 1 are constructed to have the charge localized on site A/B, and this charge localization character does not change as the reaction occurs.

In contrast to *adiabatic* states, which are the eigenstates of the electronic Hamiltonian within the Born-Oppenheimer approximation, *diabatic* states are *not* eigenstates of the electronic Hamiltonian of the whole system, and therefore are not directly accessible from standard electronic structure calculations. Constrained density functional theory (CDFT) provides a powerful and robust framework for constructing diabatic states from first principles and predicting their electronic coupling^{25,26}, including instances where hybrid functionals may fail to produce a localized state²⁷ and where time-dependent DFT may fail to produce the correct spatial decay of the electronic coupling²⁸. In CDFT, additional constraint potentials are added to the Kohn-Sham Hamiltonian, and their strengths are optimized so as to obtain a desired localized charge on a given site. To obtain the electronic coupling H_{ab} , one first performs two separate CDFT calculations in which one localizes the charge on the initial and final sites. Then, one constructs the electronic Hamiltonian matrix on the basis composed of the two diabatic states, and finally the H_{ab} is given by the off-diagonal elements of the Hamiltonian matrix.

A CDFT formulation was originally proposed by Dederichs in 1984²⁹ to study excitations of Ce impurities in metals. Wu, van Voorhis and co-workers established the modern formulation of CDFT in the mid-2000s^{30,31}. Since then it has been implemented in several DFT codes using localized basis sets, such as SIESTA³², NWChem³¹, Q-CHEM³³ and ADF³⁴.

Implementations of CDFT using plane-wave basis sets appeared more recently, for instance in CPMD^{35,36}, VASP³⁷ and CP2K (dual basis)³⁸. These plane-wave implementations enabled CDFT calculations for condensed systems, and facilitated the study of important problems such as redox couples in aqueous solution^{35,35,39}, charge transfer in biological molecules and proteins⁴⁰, in quantum dots⁴¹ and doped nanoparticles⁴², electron tunneling between defects⁴³ and polaron transport^{44,45} in oxides, molecular solids⁴⁰, and organic photovoltaic polymers⁴⁶ (see Ref. 25 and Ref. 2 for extensive reviews). In existing implementations, DFT and CDFT are developed and maintained in the same code, thus requiring direct modifications of core DFT routines to support CDFT functionalities.

In recent years, an emerging trend in scientific simulation software is the development of light-weight code, with focus on specific tasks, which can be interfaced with other codes to perform complex tasks. This strategy is well aligned with the modular programming coding practice, which enables maintainability, re-usability, and simplicity of codes. Compared to conventional strategies integrating a wide range of functionalities into one single code, this design strategy decouples the development cycle of different functionalities and leads to interoperable codes that are easier to modify and maintain, facilitating rapid developments and release of new features. Some notable codes for chemical and materials simulations that have adopted this strategy include Qbox⁴⁷, WEST^{48,49}, and SSAGES^{50,51}.

In this work we present PyCDFT, a Python package that performs single-point self-consistent-field (SCF) and geometry optimization calculations using CDFT. PyCDFT can be interfaced with existing DFT codes to perform DFT calculations with constraint potentials. Compared to existing implementations of CDFT, the novelty of the PyCDFT code is twofold:

- PyCDFT is a light-weight, interoperable code. The operations specific to CDFT calculations are decoupled from those carried out by existing DFT codes (DFT engines). Communications between PyCDFT and the DFT engine are handled by client-server interfaces (see Sec. 3). Hence, the development of PyCDFT and of the DFT engine may occur independently. This is advantageous for maintainability and reusability, and PyCDFT may be interfaced with multiple DFT engines.
- PyCDFT features an object-oriented design that is user-friendly and extensible. Extra functionalities can be easily added to PyCDFT thanks to the extensive use of abstract classes. Furthermore, PyCDFT supports being used within Jupyter notebooks or Python terminals, thus allowing users to perform and analyze CDFT calculations in a flexible and interactive manner.

We note that Python has become increasingly popular as a high-level programming language for scientific computing due to its ease of use and wide applicability. The development of PyCDFT echos this trend and contributes to the rapidly expanding open-source Python ecosystem for the molecular and materials science fields, where some widely-used packages include Atomic Simulation Environment (ASE)⁵², pymatgen⁵³, and PySCF⁵⁴.

To demonstrate the use of PyCDFT, we coupled it with the massively parallel first-principles molecular dynamics code **Qbox**⁴⁷, which features efficient DFT calculations using plane-wave basis sets and pseudopotentials. We computed diabatic electronic coupling for a set of organic molecules in the HAB18 data set^{55,56} and compared our results with those of existing implementations. The results obtained with PyCDFT(Qbox) are in good agreement with those of other plane-wave implementations of CDFT, thus verifying the correctness and robustness of PyCDFT.

2 COMPUTATIONAL METHODOLOGY

2.1 Constrained Density Functional Theory

We briefly outline the CDFT methodology adopted here and we refer the reader to Refs. 25,27,31,36,57 for further details. The core of the CDFT method is the iterative calculation of the stationary point of a free energy functional W defined as

$$W[n, V_k] = E[n] + \sum_k V_k \left(\int w_k(\mathbf{r}) n(\mathbf{r}) d\mathbf{r} - N_k^0 \right), \quad (2)$$

where n is the electron density; $E[n]$ is the DFT total energy functional; the second term on the right-hand side of Eq. 2 represents the sum of constraint potentials applied to the system to ensure that the desired number of electrons N_k^0 is localized on given parts of the system (e.g., chosen atomic site, molecule, or structural fragment). More than one constraint can be applied to the system, if needed. The strength of the k^{th} constraint potential is controlled by the scalar Lagrange multiplier V_k , and its shape is determined by a weight function $w_k(\mathbf{r})$. CDFT calculations are performed by self-consistently minimizing W with respect to n and maximizing W with respect to V_k . The minimization of W with respect to n is equivalent to performing a DFT calculation with additional constraint potentials $\sum_k V_k w_k(\mathbf{r})$ added to the Kohn-Sham Hamiltonian. Upon convergence of the SCF cycle, the number of electrons localized on a given site $N_k = \int d\mathbf{r} w_k(\mathbf{r}) n(\mathbf{r})$ is equal to the desired value N_k^0 . In geometry optimization calculations, the free energy W is further minimized with respect to nuclear coordinates, as shown in the outermost cycle in Fig. 2.

2.2 Calculation of weight functions

The weight function allows one to partition the total electron density into contributions from different fragments of the whole system. Several different partitioning schemes have been proposed, such as Mulliken⁵⁸, Becke⁵⁹, and Hirshfeld partitioning⁶⁰. In PyCDFT we implemented the Hirshfeld partitioning, which is widely used in plane-wave implementations of CDFT^{26,55,56}. The Hirshfeld weight function w is defined as the ratio between the pseudoatomic densities belonging to a given site and the total pseudoatomic density

$$w(\mathbf{r}) = \frac{\sum_{I \in F} \rho_I(\mathbf{r} - \mathbf{R}_I)}{\sum_I \rho_I(\mathbf{r} - \mathbf{R}_I)}, \quad (3)$$

where I denotes atoms and $I \in F$ denotes atoms belonging to a fragment F to which the constraint is applied; \mathbf{R}_I is the coordinate of atom I ; ρ_I denotes the electron density of the *isolated* I -th atom and should not be confused with the electron density n of the whole system.

Alternatively, to enforce constraints on the electron number difference between a donor site D and an acceptor site A, one can define the weight function as:

$$w(\mathbf{r}) = \frac{\sum_{I \in D} \rho_I(\mathbf{r} - \mathbf{R}_I) - \sum_{I \in A} \rho_I(\mathbf{r} - \mathbf{R}_I)}{\sum_I \rho_I(\mathbf{r} - \mathbf{R}_I)}. \quad (4)$$

Both definitions of Hirshfeld weights are implemented in PyCDFT [see Sec. S3 of the supplementary information (SI)]. For charge transfer processes where the whole system consists of only two fragments (donor and acceptor), the above two definitions of Hirshfeld weights are equivalent. For more complex processes where multiple parts of the system are involved, one can use a combination of the two definitions to enforce complex charge constraints.

In Eqs. 3 and Eq. 4, the real-space electron density of an atom located at \mathbf{R}_I is computed as:

$$\rho_I(\mathbf{r} - \mathbf{R}_I) = 4\pi\mathcal{F}^{-1} \left[e^{-i\mathbf{G} \cdot \mathbf{R}_I} \int_0^\infty \rho_I(r) \frac{r \sin(Gr)}{G} dr \right], \quad (5)$$

where \mathcal{F}^{-1} denotes an inverse Fourier transform; \mathbf{G} is a reciprocal lattice vector with norm G ; $\rho_I(r)$ is the radial electron density of atom I . For a given atomic species, $\rho_I(r)$ can be easily obtained by performing DFT calculations for isolated atoms. PyCDFT is distributed with pre-computed spherically-averaged electron densities obtained with the SG15 pseudopotentials^{61,62} for all species in the periodic table before bismuth (excluding the lanthanides).

2.3 Calculation of Forces

In order to perform geometry optimizations or molecular dynamics simulations on a diabatic potential energy surface, the force on each nucleus due to the applied constraints must be evaluated. Forces on the diabatic potential energy surface are the sum of the DFT forces F^{DFT} and the constraint force F^c arising from the derivative of the constraint potential with respect to nuclear coordinates.

For a system subject to constraints, the α component ($\alpha \in \{x, y, z\}$) of the constraint force F^c on the I^{th} atom is given by:

$$\begin{aligned} F_{I\alpha}^c &= - \sum_k V_k \int d\mathbf{r} \rho(\mathbf{r}) \frac{\partial w_k(\mathbf{r})}{\partial R_{I\alpha}} \\ &= - \sum_k V_k \int d\mathbf{r} \rho(\mathbf{r}) \frac{\delta - w_k(\mathbf{r})}{\sum_J \rho_J(\mathbf{r} - \mathbf{R}_J)} \frac{\partial \rho_I(\mathbf{r} - \mathbf{R}_I)}{\partial R_{I\alpha}}, \end{aligned} \quad (6)$$

where $\delta = \delta_{I \in F}$ for constraints on absolute electron numbers (Eq. 3) and $\delta = \delta_{I \in D} - \delta_{I \in A}$ for constraints on electron number differences (Eq. 4). The term $\frac{\partial \rho_I(\mathbf{r} - \mathbf{R}_I)}{\partial R_{I\alpha}}$ is evaluated as:

$$\frac{\partial \rho_I(\mathbf{r} - \mathbf{R}_I)}{\partial R_{I\alpha}} = \mathcal{F}^{-1} \left\{ -i G_\alpha e^{-i\mathbf{G} \cdot \mathbf{R}_I} \mathcal{F}[\rho_I(\mathbf{r})] \right\}, \quad (7)$$

where \mathcal{F} and \mathcal{F}^{-1} denote forward and backward Fourier transforms, respectively. In Sec. S3 of the SI, we verify the analytical calculation of forces using Eq. 6 and Eq. 7 by comparing with results obtained with finite difference calculations of total energies.

2.4 Diabatic electronic coupling

To compute the electronic coupling H_{ab} ³⁰, we consider the Hamiltonian matrix on the diabatic basis composed of two diabatic states Ψ_a and Ψ_b , each obtained from a converged CDFT calculation with PyCDFT. Here we consider the case of a single constraint. Denoting the value of the Lagrange multiplier for the two CDFT calculations as V_a and V_b , respectively, the Hamiltonian on the diabatic basis is:

$$\mathbf{H} = \begin{pmatrix} H_{aa} & H_{ab} \\ H_{ba} & H_{bb} \end{pmatrix}, \quad (8)$$

where the diagonal elements H_{aa} and H_{bb} correspond to the DFT total energies of diabatic states Ψ_a and Ψ_b , respectively. Then, denoting the overlap matrix \mathbf{S} between the two diabatic states as

$$\mathbf{S} = \begin{pmatrix} 1 & S_{ab} \\ S_{ba} & 1 \end{pmatrix}, \quad (9)$$

where $S_{ab} = \langle \Psi_a | \Psi_b \rangle$ and $S_{ba} = S_{ab}^*$, the off-diagonal Hamiltonian elements can be written as³⁶:

$$H_{ab} = F_b S_{ab} - V_b W_{ab} \quad (10)$$

$$H_{ba} = F_a S_{ba} - V_a W_{ba} \quad (11)$$

where F_a and F_b are the CDFT total energies including the contribution of constraint potentials; the weight function matrix elements $W_{ab} = W_{ba}^*$ are given by $W_{ab} = \langle \Psi_a | w(\mathbf{r}) | \Psi_b \rangle$.

After \mathbf{H} is evaluated in the diabatic basis, we follow Ref. 36 and average the off-diagonal elements of \mathbf{H} to ensure its Hermiticity. Finally, we perform a Löwdin orthogonalization⁶³ for \mathbf{H} using the overlap matrix \mathbf{S}

$$\tilde{\mathbf{H}} = \mathbf{S}^{-1/2} \mathbf{H} \mathbf{S}^{-1/2} \quad (12)$$

and the off-diagonal matrix element of $\tilde{\mathbf{H}}$ corresponds to the electronic coupling H_{ab} .

3 Software

Implementation

PyCDFT features an object-oriented design and extensive use of abstract classes and abstract methods to facilitate future extensions of functionalities. Here we list the major classes defined in the PyCDFT package.

- **Sample**: a container class to organize relevant information about the physical system. A **Sample** instance is constructed by specifying the positions of the atoms within the periodic cell. The **Sample** class utilizes the ASE⁵² package to parse atomic structures from geometry files (e.g., `cif` files).

- **Fragment**: a container class to represent a part of the whole system to which constraints are applied. A **Fragment** instance is constructed by specifying a list of atoms belonging to the fragment.
- **Constraint**: an abstract class representing a constraint applied to the system. A **Constraint** instance keeps track of physical quantities relevant to the constraint, such as N_k^0 , N_k , V_k , and $w_k(\mathbf{r})$ (see Eq. 2). Except for the parameter N_k^0 , which is defined upon the construction of the instance, other quantities are updated self-consistently as the CDFT calculation proceeds. Currently, two types of constraints based on Hirshfeld partitioning are implemented: **ChargeConstraint** (Eq. 3) and **ChargeTransferConstraint** (Eq. 4).
- **DFTDriver**: an abstract class that controls how PyCDFT interacts with an external DFT code. It specifies how PyCDFT communicates the constraint potentials and constraint forces to the DFT code and how to fetch the charge densities and other relevant quantities from the DFT code. Currently, a subclass **QboxDriver** is implemented, which allows PyCDFT to interact with the **Qbox** code. The implementation of the **QboxDriver** class leverages the client-server interface of **Qbox**, which allows **Qbox** to interactively respond to commands provided by a user or an external code^{64,65} (PyCDFT in this case).
- **CDFTSolver**: the core class of PyCDFT that executes a CDFT calculations. **CDFTSolver** provides a **solve** method, which is used to perform a CDFT self-consistent or geometry optimization calculation. Optimization of the Lagrange multipliers is performed within the **solve** method, which utilizes the **scipy** package.

In addition to the above classes, PyCDFT contains a `compute_elcoupling` function, which takes two **CDFTSolver** instances as input and computes the electronic coupling H_{ab} between two diabatic states (see Sec. 2.4). To enable the calculation of electronic coupling, PyCDFT implements an auxiliary **Wavefunction** class that stores and manipulates the Kohn-Sham orbitals from CDFT calculations.

Extensibility

Thanks to the use of abstract classes, `PyCDFT` can be easily extended to provide new functionalities. For instance, support for additional weight functions (such as spin-dependent weight functions) can be easily implemented by defining subclasses of `Constraint` and overriding its abstract methods. Similarly, one can extend `PyCDFT` to support other DFT codes by overriding the abstract methods in the `DFTDriver` class. In addition to the C++ code `Qbox` used here, several Python implementations of DFT (e.g., `PySCF`) may be called as a DFT driver in an interactive manner; therefore they may be used as DFT drivers of `PyCDFT` once the corresponding `DFTDriver` subclass is implemented.

`PyCDFT` may also be readily integrated with existing Python-based interfaces for generating, executing, and analyzing electronic structure calculations using software such as `ASE`⁵² and `Atomate`⁶⁶.

3.1 Installation and usage

Installation of `PyCDFT` follows the standard procedure using the `setup.py` file included in the distribution. Currently, it depends on a few readily available Python packages including `ASE`, `scipy`, `pyFFTW`, and `lxml`.

In Fig. 3 we present an example script that utilizes `PyCDFT` to compute the diabatic electronic coupling for the helium dimer He_2^+ . This and other examples are included in the distribution of `PyCDFT`.

4 Verification

We now turn to the verification of our implementation of CDFT in `PyCDFT`, focusing on the calculation of electronic couplings. We compare results obtained with `PyCDFT(Qbox)`, `CPMD`^{36,55,56}), `CP2K`, and the implementation of CDFT in `QUANTUM ESPRESSO`⁶⁷ originally contributed by Goldey et al.²⁶. We note that all codes utilized for this comparison use plane-wave basis sets, with the exception of `CP2K`, which uses a mixed Gaussian and plane-wave basis set. As the values obtained for the electronic coupling have been shown

to be sensitive to the choice of weight partitioning schemes³⁶, we compare with only results obtained with the Hirshfeld partitioning scheme.

Our results, PyCDFT(Qbox), are obtained by performing DFT calculations with the Qbox⁴⁷ code. We used optimized norm-conserving Vanderbilt pseudopotentials (ONCV)^{61,62}, and an energy cutoff of 40 Ry for all molecules; we tested up to a 90 Ry energy cutoff and found changes of 1-2% in the electronic coupling compared to calculations using a 40 Ry cutoff. We used a convergence threshold of 5×10^{-5} for $|N - N_0|$. The electronic couplings were converged to within less than 0.5% with respect to cell size, in order to minimize interactions with periodic images. When using CP2K, we adopted the TZV2P basis set with GTH pseudopotentials⁶⁸. Results obtained with QUANTUM ESPRESSO (QE) and CPMD have been previously reported in Ref. 26 and Refs. 55,56, respectively. In all cases the DFT electronic structure problem was solved using the generalized gradient approximation of Perdew, Burke, and Ernzerhof (PBE)⁶⁹.

We first discuss results for the electronic coupling of the He_2^+ dimer. Figure 4 compares the decay in H_{ab} with distance for hole transfer in the He-He⁺ dimer obtained with PyCDFT(Qbox) and other codes. We find excellent agreement between our computed electronic couplings and those from Oberhofer and Blumberger³⁶ obtained using CPMD and the results of Goldey et al.²⁶ obtained using QE. As wavefunctions decay exponentially, the variation of the electronic coupling with separation may be expressed as $H \propto \exp(-\beta R/2)$, and we can compare the decay behaviors obtained here and in the literature by using the decay rate β , which is found to be 4.64, 4.98, 4.13 1/Å with PyCDFT(Qbox), CPMD, and QUANTUM ESPRESSO (QE), respectively.

We now turn to bench-marking results for molecular dimers in the HAB18 dataset, which combines the HAB11⁵⁵ and HAB7⁵⁶ data sets, and consists of π -stacked organic homo-dimers. The molecules in the HAB11 data set contain members with different number of π -bonds and atomic species; the HAB7 dataset contains larger molecules. The combined HAB18 data set has been previously used for other implementations of CDFT²⁶. The first molecule we consider here is one where imperfect π -stacking is present, due to one of the monomers being rotated relative to the other. Fig. 5 compares our calculated electron coupling for this configuration of the thiophene dimer with that of Kubas et al as implemented

in CPMD⁵⁵. We find excellent agreement between the two results, thus demonstrating the accuracy and robustness of PyCDFT(Qbox) for off-symmetry configurations.

Next we analyze in greater detail the performance of PyCDFT(Qbox) compared to CP2K, CPMD, and Quantum Espresso implementations for other members of the HAB18 data set for perfectly π -stacked homo-dimers. In the appendix, Table S1 (see SI) shows the calculated electronic couplings for molecular dimers as a function of inter-molecular distance. Tables S2 and S3 report the mean error, mean absolute error, root-mean-square deviation, and mean absolute percent error among codes for the electronic coupling and decay constants, respectively.

We compare our computed electronic couplings of molecular dimers in the HAB18 data set at varying intermolecular distances using PyCDFT(Qbox) with those obtained with CP2K, CPMD, and QE. These are plotted in Fig. 6 on a log-log scale. In general, there is good agreement among the various codes. There is a systematic deviation of all DFT results from those based on multi-reference configuration interaction (MRCI+Q)⁵⁵ and single-determinant spin-component-scaled coupled cluster (SCS-CC2)⁵⁶ calculations. This systematic deviation arises from the well-known delocalization error of the semi-local functional used here (PBE) and from its shortcoming to properly describe long-range dispersion interactions. Using more accurate functionals would improve the accuracy of CDFT, as previously reported in the literature⁵⁶. Nevertheless, inspection of Fig. 6 (and Table S1) shows that PyCDFT(Qbox) generally yields electronic couplings and decay constants within the range of values obtained from previous implementations. Finally, we emphasize that PyCDFT(Qbox) captures the physically relevant exponential decay of the electronic coupling with intermolecular distance.

5 CONCLUSIONS

In this work we presented PyCDFT, a Python module for performing calculations based on constrained density function theory (CDFT). PyCDFT allows for SCF and geometry optimization calculations of diabatic states, as well as calculations of diabatic electronic couplings. The implementation of CDFT in PyCDFT is flexible and modular, and enables ease of use, maintenance, and effective dissemination of the code. Using molecules from the HAB18

data set^{55,56} as benchmarks, we demonstrated that PyCDFT(Qbox) yields results in good agreement with those of existing CDFT implementations using plane-wave basis sets and pseudopotentials. As a robust implementation for CDFT calculations, PyCDFT is well-suited for first-principles studies of charge transfer processes.

ACKNOWLEDGMENTS

We thank Francois Gygi for helpful discussions. We thank Chenghan Li for generous help with calculations using CP2K. H.M., M.G. and G.G. are supported by MICCoM, as part of the Computational Materials Sciences Program funded by the U.S. Department of Energy, Office of Science, Basic Energy Sciences, Materials Sciences and Engineering Division through Argonne National Laboratory, under contract number DE-AC02-06CH11357. W.W. is supported by the National Science Foundation (NSF) under Grant No. CHE-1764399. S.K. was supported by DOE/BES under grant no. de-sc0012405. This research used computational resources of the University of Chicago Research Computing Center.

References

1. V. May and O. Kühn, *Charge and energy transfer dynamics in molecular systems*, vol. 2 (Wiley Online Library, 2011).
2. J. Blumberger, Chemical Reviews **115**, 11191 (2015), ISSN 0009-2665, 1520-6890.
3. M. D. Newton and N. Sutin, Annual Review of Physical Chemistry **35**, 437 (1984).
4. Y. Jiang, H. Geng, W. Li, and Z. Shuai, Journal of chemical theory and computation **15**, 1477 (2019).
5. Y. Jiang, Q. Peng, H. Geng, H. Ma, and Z. Shuai, Physical Chemistry Chemical Physics **17**, 3273 (2015).
6. J. J. Hopfield, Proceedings of the National Academy of Sciences **71**, 3640 (1974), ISSN 0027-8424, 1091-6490.
7. M. L. Jones, I. V. Kurnikov, and D. N. Beratan, The Journal of Physical Chemistry A **106**, 2002 (2002), ISSN 1089-5639, 1520-5215.
8. X. Zeng, X. Hu, and W. Yang, Journal of Chemical Theory and Computation **8**, 4960 (2012), ISSN 1549-9618, 1549-9626.
9. N. Gillet, L. Berstis, X. Wu, F. Gajdos, A. Heck, A. de la Lande, J. Blumberger, and M. Elstner, Journal of Chemical Theory and Computation **12**, 4793 (2016), ISSN 1549-9618, 1549-9626.
10. H. Yamada and K. Iguchi, Advances in Condensed Matter Physics **2010**, 1 (2010), ISSN 1687-8108, 1687-8124.
11. C. Schober, K. Reuter, and H. Oberhofer, The Journal of Chemical Physics **144**, 054103 (2016), ISSN 0021-9606, 1089-7690.
12. H. Oberhofer, K. Reuter, and J. Blumberger, Chemical Reviews **117**, 10319 (2017), ISSN 0009-2665, 1520-6890.

13. Z. Shuai, L. Wang, and C. Song, *Theory of charge transport in carbon electronic materials* (Springer Science & Business Media, 2012).
14. H. Bässler and A. Köhler, in *Unimolecular and Supramolecular Electronics I: Chemistry and Physics Meet at Metal-Molecule Interfaces*, edited by R. M. Metzger (Springer Berlin Heidelberg, Berlin, Heidelberg, 2012), pp. 1–65, ISBN 978-3-642-27284-4.
15. X. Lan, M. Chen, M. H. Hudson, V. Kamysbayev, Y. Wang, P. Guyot-Sionnest, and D. V. Talapin, *Nature Materials* **19**, 323 (2020), ISSN 1476-1122, 1476-4660.
16. D. V. Talapin, J.-S. Lee, M. V. Kovalenko, and E. V. Shevchenko, *Chemical Reviews* **110**, 389 (2010), ISSN 0009-2665, 1520-6890.
17. P. Guyot-Sionnest, *The Journal of Physical Chemistry Letters* **3**, 1169 (2012), ISSN 1948-7185.
18. D. Yu, C. Wang, B. L. Wehrenberg, and P. Guyot-Sionnest, *Physical Review Letters* **92** (2004), ISSN 0031-9007, 1079-7114.
19. R. A. Marcus, *The Journal of Chemical Physics* **24**, 966 (1956), ISSN 0021-9606, 1089-7690.
20. R. A. Marcus, *Reviews of Modern Physics* **65**, 599 (1993), ISSN 0034-6861, 1539-0756.
21. L. Landau, *Phys. Z. Sowjetunion* **1**, 88 (1932).
22. C. Zener, *Proceedings of the Royal Society A: Mathematical, Physical and Engineering Sciences* **137**, 696 (1932), ISSN 1364-5021, 1471-2946.
23. S. Lin, C. Chang, K. Liang, R. Chang, J. Zhang, T. Yang, M. Hayashi, Y. Shiu, and F. Hsu, *Advances in chemical physics* **121**, 1 (2002).
24. G. Nan, X. Yang, L. Wang, Z. Shuai, and Y. Zhao, *Physical Review B* **79**, 115203 (2009).
25. B. Kaduk, T. Kowalczyk, and T. Van Voorhis, *Chemical Reviews* **112**, 321 (2012), ISSN 0009-2665, 1520-6890.

26. M. B. Goldey, N. P. Brawand, M. Vörös, and G. Galli, *Journal of Chemical Theory and Computation* **13**, 2581 (2017), ISSN 1549-9618, 1549-9626.
27. M. Melander, E. Ö. Jónsson, J. J. Mortensen, T. Vegge, and J. M. García Lastra, *Journal of Chemical Theory and Computation* **12**, 5367 (2016), ISSN 1549-9618, 1549-9626.
28. A. Dreuw and M. Head-Gordon, *Journal of the American Chemical Society* **126**, 4007 (2004), ISSN 0002-7863, 1520-5126.
29. P. H. Dederichs, S. Blügel, R. Zeller, and H. Akai, *Physical Review Letters* **53**, 2512 (1984), ISSN 0031-9007.
30. Q. Wu and T. Van Voorhis, *The Journal of Chemical Physics* **125**, 164105 (2006), ISSN 0021-9606, 1089-7690.
31. Q. Wu and T. Van Voorhis, *The Journal of Physical Chemistry A* **110**, 9212 (2006), ISSN 1089-5639, 1520-5215.
32. A. M. Souza, I. Rungger, C. D. Pemmaraju, U. Schwingenschloegl, and S. Sanvito, *Physical Review B* **88** (2013), ISSN 1098-0121, 1550-235X.
33. Q. Wu, B. Kaduk, and T. Van Voorhis, *The Journal of Chemical Physics* **130**, 034109 (2009), ISSN 0021-9606, 1089-7690.
34. G. te Velde, F. M. Bickelhaupt, E. J. Baerends, C. Fonseca Guerra, S. J. A. van Gisbergen, J. G. Snijders, and T. Ziegler, *J. Comput. Chem.* **22**, 931 (2001), ISSN 1096-987X, URL <http://dx.doi.org/10.1002/jcc.1056>.
35. H. Oberhofer and J. Blumberger, *The Journal of Chemical Physics* **131**, 064101 (2009), ISSN 00219606.
36. H. Oberhofer and J. Blumberger, *The Journal of Chemical Physics* **133**, 244105 (2010), ISSN 0021-9606, 1089-7690.
37. P.-W. Ma and S. L. Dudarev, *Physical Review B* **91** (2015), ISSN 1098-0121, 1550-235X.

38. J. Hutter, M. Iannuzzi, F. Schiffman, and J. VandeVondele, WIREs Computational Molecular Science **4**, 15 (2014).
39. J. Blumberger, I. Tavernelli, M. L. Klein, and M. Sprik, The Journal of Chemical Physics **124**, 064507 (2006), ISSN 0021-9606, 1089-7690.
40. H. Oberhofer and J. Blumberger, Physical Chemistry Chemical Physics **14**, 13846 (2012), ISSN 1463-9076, 1463-9084.
41. N. P. Brawand, M. B. Goldey, M. Vörös, and G. Galli, Chemistry of Materials **29**, 1255 (2017), ISSN 0897-4756, 1520-5002.
42. M. Vörös, N. P. Brawand, and G. Galli, Chemistry of Materials **29**, 2485 (2017), ISSN 0897-4756, 1520-5002.
43. J. Blumberger and K. P. McKenna, Physical Chemistry Chemical Physics **15**, 2184 (2013), ISSN 1463-9076, 1463-9084.
44. H. Seo, Y. Ping, and G. Galli, Chemistry of Materials **30**, 7793 (2018).
45. W. Wang, P. Strohbeen, D. Lee, C. Zhou, J. Kawasaki, K.-S. Choi, M. Liu, and G. Galli, Chemistry of Materials **Just accepted**. (2020).
46. M. B. Goldey, D. Reid, J. de Pablo, and G. Galli, Physical Chemistry Chemical Physics **18**, 31388 (2016), ISSN 1463-9076, 1463-9084.
47. F. Gygi, IBM Journal of Research and Development **52**, 137 (2008), ISSN 0018-8646, 0018-8646.
48. M. Govoni and G. Galli, Journal of Chemical Theory and Computation **11**, 2680 (2015), ISSN 1549-9618, 1549-9626.
49. H. Ma, M. Govoni, F. Gygi, and G. Galli, Journal of chemical theory and computation **15**, 154 (2018).
50. H. Sidky, Y. J. Colón, J. Helfferich, B. J. Sikora, C. Bezik, W. Chu, F. Giberti, A. Z. Guo, X. Jiang, J. Lequieu, et al., The Journal of chemical physics **148**, 044104 (2018).

51. E. Sevgen, F. Giberti, H. Sidky, J. K. Whitmer, G. Galli, F. Gygi, and J. J. de Pablo, *Journal of Chemical Theory and Computation* **14**, 2881 (2018), ISSN 1549-9618, 1549-9626.
52. A. Hjorth Larsen, J. Jørgen Mortensen, J. Blomqvist, I. E. Castelli, R. Christensen, M. Dułak, J. Friis, M. N. Groves, B. Hammer, C. Hargus, et al., *Journal of Physics: Condensed Matter* **29**, 273002 (2017), ISSN 0953-8984, 1361-648X.
53. S. P. Ong, W. D. Richards, A. Jain, G. Hautier, M. Kocher, S. Cholia, D. Gunter, V. L. Chevrier, K. A. Persson, and G. Ceder, *Computational Materials Science* **68**, 314 (2013), ISSN 09270256.
54. Q. Sun, T. C. Berkelbach, N. S. Blunt, G. H. Booth, S. Guo, Z. Li, J. Liu, J. D. McClain, E. R. Sayfutyarova, S. Sharma, et al., *Wiley Interdisciplinary Reviews: Computational Molecular Science* **8**, e1340 (2018).
55. A. Kubas, F. Hoffmann, A. Heck, H. Oberhofer, M. Elstner, and J. Blumberger, *The Journal of Chemical Physics* **140**, 104105 (2014), ISSN 0021-9606, 1089-7690.
56. A. Kubas, F. Gajdos, A. Heck, H. Oberhofer, M. Elstner, and J. Blumberger, *Physical Chemistry Chemical Physics* **17**, 14342 (2015), ISSN 1463-9076, 1463-9084.
57. Q. Wu and T. Van Voorhis, *Physical Review A* **72**, 024502 (2005), ISSN 1050-2947, 1094-1622.
58. R. S. Mulliken, *The Journal of Chemical Physics* **23**, 1833 (1955), ISSN 0021-9606, 1089-7690.
59. A. D. Becke, *The Journal of Chemical Physics* **88**, 2547 (1988), ISSN 0021-9606, 1089-7690.
60. F. L. Hirshfeld, *Theoretica Chimica Acta* **44**, 129 (1977), ISSN 0040-5744, 1432-2234.
61. D. R. Hamann, *Physical Review B* **88**, 085117 (2013), ISSN 1098-0121, 1550-235X.
62. M. Schlipf and F. Gygi, *Computer Physics Communications* **196**, 36 (2015), ISSN 00104655.

- 63. P.-O. Löwdin, The Journal of Chemical Physics **18**, 365 (1950), ISSN 0021-9606, 1089-7690.
- 64. H. Ma, M. Govoni, F. Gygi, and G. Galli, Journal of chemical theory and computation **15**, 154 (2018).
- 65. N. L. Nguyen, H. Ma, M. Govoni, F. Gygi, and G. Galli, Physical review letters **122**, 237402 (2019).
- 66. K. Mathew, J. H. Montoya, A. Faghaninia, S. Dwarakanath, M. Aykol, H. Tang, I.-h. Chu, T. Smidt, B. Bocklund, M. Horton, et al., Computational Materials Science **139**, 140 (2017).
- 67. P. Giannozzi, O. Andreussi, T. Brumme, O. Bunau, M. Buongiorno Nardelli, M. Calandra, R. Car, C. Cavazzoni, D. Ceresoli, M. Cococcioni, et al., Journal of Physics: Condensed Matter **29**, 465901 (2017), ISSN 0953-8984, 1361-648X.
- 68. S. Goedecker, M. Teter, and J. Hutter, Physical Review B **54**, 1703 (1996).
- 69. J. P. Perdew, K. Burke, and M. Ernzerhof, Physical Review Letters **77**, 3865 (1996), ISSN 0031-9007, 1079-7114.

Figure 1: Free energy curves for two diabatic states Ψ_a and Ψ_b with free energy G_a and G_b associated to a reaction where a charge (electron or hole) is transferred from site A to site B. The charge is localized on site A for Ψ_a and site B for Ψ_b , and the charge localization characters of Ψ_a and Ψ_b do not change as the reaction occurs. The charge transfer rate can be written as a function of the free energy difference ΔG , reorganization energy λ , and electronic coupling H_{ab} (see text).

Figure 2: Workflow for self-consistent-field (SCF) and geometry optimization calculations performed by PyCDFT. In SCF calculations, the free energy functional W is minimized with respect to the electron density n (equivalent to a standard DFT calculation under constraint potentials) and maximized with respect to Lagrange multipliers V_k . For geometry optimization calculations, W is further minimized with respect to nuclear coordinates \mathbf{R} . PyCDFT is designed to implement CDFT-specific algorithms and to be interfaced with external DFT codes (drivers).

Figure 3: An example Python script to perform CDFT calculations for He_2^+ . Two `CDFTSolver` instances are created for the calculation of two diabatic states with different charge localization, then the `compute_elcoupling` function is called to compute the electronic coupling H_{ab} between the two diabatic states.

Figure 4: Comparison of diabatic electronic coupling H_{ab} of the He-He⁺ dimer as a function of distance R , calculated with constrained density functional theory, and using PyCDFT interfaced with the Qbox code (PyCDFT(Qbox)), the implementation of CDFT in CPMD from Oberhofer and Blumberger³⁶, and the implementation in QUANTUM ESPRESSO (QE) from Goldey et al²⁶. In all implementations, the Hirshfeld partitioning⁶⁰ scheme is used. The calculated β decay rates are 4.64, 4.98, and 4.13 1/Å respectively.

Figure 5: Diabatic electronic coupling H_{ab} of the stacked thiophene dimer at a separation of 5 Å as a function of the relative rotation of the two units, calculated with constrained density functional theory as implemented in this work (PyCDFT(Qbox)) and in Kubas et al in CPMD⁵⁵. Carbon atoms are shown in brown, sulfur in yellow, and hydrogen in beige.

Figure 6: Log-log plot of computed diabatic electronic couplings for molecular dimers in the HAB18 data set^{55,56} at various inter-molecular distances using PyCDFT(Qbox) (blue circles), CP2K (purple stars), CPMD (green squares), and Quantum Espresso (QE, yellow triangles). Reference values (black line) are based on multi-reference configuration interaction (MRCI+Q)⁵⁵ and single-determinant spin-component-scaled coupled cluster (SCS-CC2)⁵⁶ level of theory.

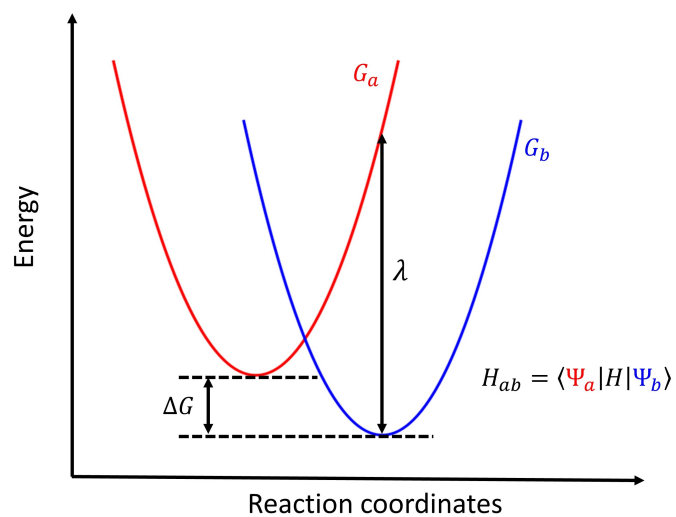


Figure 1
 He Ma, Wennie Wang, Siyoung
 Kim, Man-Hin Cheng, Marco
 Govoni, Giulia Galli
 J. Comput. Chem.


```

# An example input for computing electronic coupling of He2+ dimer

from pycdft import *
from ase.io import read

# Read atomic structure
cell = read("./He2.cif")

# Construct sample class, set FFT grid
sample = Sample(ase_cell=cell, n1=112, n2=112, n3=112)

# Set up the DFT driver, provide necessary commands to initialize
# the external DFT code (Qbox in this case)
qboxdriver = QboxDriver(
    sample=sample,
    init_cmd="load gs.xml\nset xc PBE\n"
    scf_cmd="run 0 50 5",
)

# Set up two CDFT solvers for two diabatic states
solver1 = CDFTSolver(
    job="scf", # Indicate the calculation is an SCF calculation
    optimizer="brenth", # Specify the optimizer used for the Lagrangian multiplier
    sample=sample,
    dft_driver=qboxdriver
)
solver2 = solver1.copy()

# Initialize two constraints that localize the extra +1 charge on each site
# Here we use ChargeTransferConstraint, which constrains the relative electron number
# between two Fragments that represent donor and acceptor
ChargeTransferConstraint(
    sample=solver1.sample,
    donor=Fragment(solver1.sample, solver1.sample.atoms[0:1]), # Donor fragment
    acceptor=Fragment(solver1.sample, solver1.sample.atoms[1:2]), # Acceptor fragment
    V_brak=(-1, 1), # Search region for the brenth optimizer
    N0=1, # Desired charge to be localized
)
ChargeTransferConstraint(
    sample=solver2.sample,
    donor=Fragment(solver2.sample, solver2.sample.atoms[0:1]),
    acceptor=Fragment(solver2.sample, solver2.sample.atoms[1:2]),
    V_brak=(-1, 1),
    N0=-1,
)

# Perform CDFT calculations
solver1.solve()
solver2.solve()

# Compute the electronic coupling between the two diabatic states obtained
compute_elcoupling(solver1, solver2)

```

Figure 3
He Ma, Wennie Wang, Siyoung
Kim, Man-Hin Cheng, Marco
Govoni, Giulia Galli
J. Comput. Chem.

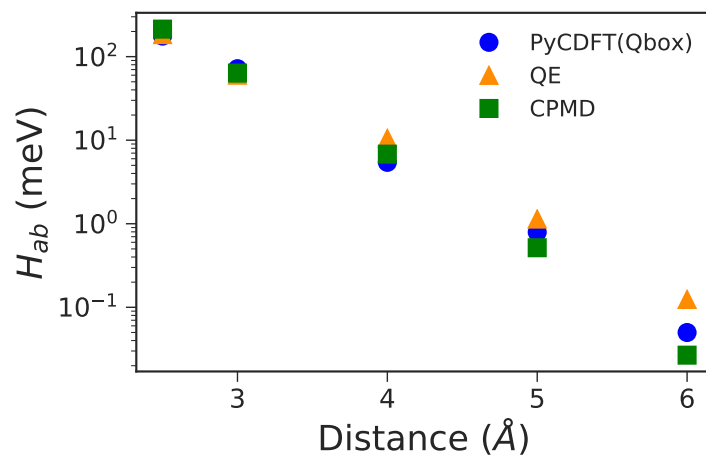


Figure 4
 He Ma, Wennie Wang, Siyoung
 Kim, Man-Hin Cheng, Marco
 Govoni, Giulia Galli
 J. Comput. Chem.

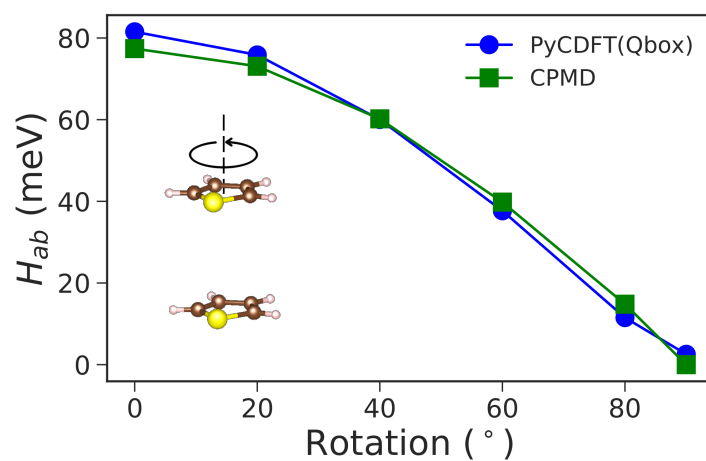


Figure 5
 He Ma, Wennie Wang, Siyoung
 Kim, Man-Hin Cheng, Marco
 Govoni, Giulia Galli
 J. Comput. Chem.

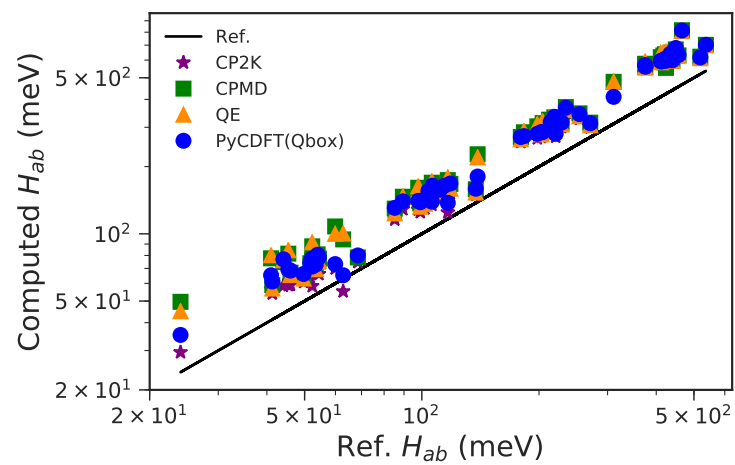


Figure 6
 He Ma, Wennie Wang, Siyoung
 Kim, Man-Hin Cheng, Marco
 Govoni, Giulia Galli
 J. Comput. Chem.